

AN EFFICIENT GENERALIZATION OF THE RUSH-LARSEN METHOD FOR SOLVING ELECTRO-PHYSIOLOGY MEMBRANE EQUATIONS*

MAURO PEREGO[†] AND ALESSANDRO VENEZIANI[‡]

Abstract. In this paper we describe a class of second-order methods for solving ordinary differential systems coming from some problems in electro-physiology. These methods extend to the second order of accuracy a previous proposal by Rush and Larsen [IEEE Trans. Biomed. Eng., 25 (1978), pp. 389–392] for the same problem. The methods can be regarded in the general framework of exponential integrators following the definition of Minchev and Wright [NTNU Tech. Report 2/05 (2005)]. However, they do differ from other schemes in this class for the specific form of linearization we pursue. We investigate the accuracy, stability, and positivity properties of our methods. Under simplifying assumptions on the problem at hand, our methods reduce to classical multi-step methods. However, we show that in general the new methods have better stability and positivity properties than the classical ones. We present a time-adaptive formulation which is well suited for our electro-physiology problems. In particular, numerical results are presented for the Monodomain model coupled to Luo-Rudy I ionic model for the propagation of the cardiac potential.

Key words. nonlinear ordinary differential systems, electro-physiology, Rush-Larsen scheme, time-adaptivity

AMS subject classifications. 65M12, 65L05, 35K65

1. Introduction. In this paper we propose a numerical method designed to solve systems of Ordinary Differential Equations (ODEs) coming from cell-membrane models for ionic currents and voltages. Starting from the Hodgkin-Huxley model [11], developed in 1952 to describe the action potential in giant squid axons, several cell-membrane models have been developed, in particular for cardiac cells. We mention, for instance, the Beeler-Reuter model [1], the Luo-Rudy phase I model [17] and the Winslow model [14] developed for the ventricular cells, and the Courtemanche model [4] for the atrial cells. All these models can be written in terms of the transmembrane potential u , the vector of the gating variables \mathbf{w} and the vector of the ionic concentrations \mathbf{X} , as follows,

$$(1.1) \quad \begin{cases} \frac{\partial u}{\partial t} = I(t, u, \mathbf{X}, \mathbf{w}), \\ \frac{\partial w_i}{\partial t} = a_i(u)w_i + b_i(u), \quad i = 1, \dots, m, \\ \frac{\partial \mathbf{X}}{\partial t} = \mathbf{g}(u, \mathbf{X}, \mathbf{w}), \end{cases}$$

for $t \in (0, T]$, with initial conditions $u(0) = u^0$, $\mathbf{w}(0) = \mathbf{w}^0$ and $\mathbf{X}(0) = \mathbf{X}^0$. $I(t, u, \mathbf{X}, \mathbf{w})$ is the source term defined as $I(t, u, \mathbf{X}, \mathbf{w}) = \frac{1}{C_m} (I_{app}(t) - I_{ion}(u, \mathbf{X}, \mathbf{w}))$, where C_m is the membrane capacity, I_{app} is an applied current stimulus, and I_{ion} is the ionic current. I_{ion} , \mathbf{g} , \mathbf{a} , \mathbf{b} , u_0 , \mathbf{w}_0 and \mathbf{X}_0 depend on the specific ionic model; in the case of Luo-Rudy phase I model, see Appendix A for functions and parameters definitions and Figure 1.1 for the graphs of the variables. Functions \mathbf{a} and \mathbf{b} of the potential u fulfill the following inequalities: $a_i < 0$, and $\left(-\frac{b_i}{a_i}\right) \in [0, 1]$. Moreover $\mathbf{w}_i^0 \in [0, 1]$ for $i = 1, \dots, m$. This

*Received January 27, 2009. Accepted for publication September 29, 2009. Published online on December 31, 2009. Recommended by K. Burrage.

[†]MOX (Modeling and Scientific Computing), Dipartimento di Matematica “F. Brioschi”, Politecnico di Milano, Italy and Department of Mathematics and Computer Science, Emory University, Atlanta, GA, USA (mauro@mathcs.emory.edu).

[‡]Department of Mathematics and Computer Science, Emory University, Atlanta, GA, USA (ale@mathcs.emory.edu).

implies that $w_i \in [0, 1]$; see Section 3.4. Typically, the system (1.1) is stiff and the gating variables feature high gradients. The most popular method for solving this system in the computational electro-cardiology community is the simple first order scheme proposed by Rush and Larsen [25] which guarantees that the numerical solutions for gating variables are in the range $[0, 1]$. In the same paper Rush and Larsen proposed a very simple time adaptive algorithm, based merely on the values of $\frac{\partial u}{\partial t}$. Another popular way to solve system (1.1) is to use the more complex Runge-Kutta (RK) schemes. Here we present a second order extension of the Rush-Larsen scheme and a time adaptive strategy based on predictor-corrector error estimates. Following the definition of *exponential integrators* advocated¹ in [18], our schemes fall into this class. However, these schemes originate from a peculiar linearization of the original problem (1.1) (that is neither linear nor semi-linear) which makes them different from other methods in this class, such as Lawson or exponential time differencing methods.

In order to simulate the action potential propagation in the myocardium, ionic models in the form (1.1) need to be coupled with the so-called Monodomain or Bidomain systems of Partial Differential Equations (PDEs). For an introduction to these models, see, e.g., [22]. Monodomain and Bidomain systems are commonly discretized using an IMplicit-EXplicit (IMEX) approach for the PDEs and the Rush-Larsen or RK schemes for the ionic model; see [5, 7]. In [23, 26] a second order method based on an operator-splitting technique was proposed for the time discretization of the PDEs, while a RK scheme was used for discretizing the ionic model. More complex time and space adaptive methods are presented in [3, 6, 29]. We solve the coupled problem with a second order IMEX scheme combined with our extended Rush-Larsen scheme for the ionic model. Time adaptive strategy for the coupled problem is extended as well. One dimensional simulations, using Finite Element discretization, are reported for the solution of Monodomain system, illustrating the effectiveness of our method.

The outline of the paper is as follows. In Section 2 we recall the Rush-Larsen method and present our extension. Section 3 is devoted to the theoretical analysis of the new method. We investigate convergence, absolute stability regions, and positivity properties. Our scheme can be viewed as a generalization of first and second order multistep methods. We prove that our generalization guarantees better stability and positivity properties. Section 4 describes some practical details on using the new scheme for the electro-physiology equations. Section 5 presents the time-adaptive formulation of our method. Numerical results for the Monodomain problem in electro-cardiology are presented in Section 6. Throughout the paper, bold characters denote vectors.

2. The scheme. For the sake of simplicity we introduce our schemes for the following scalar initial value problem,

$$(2.1) \quad \begin{cases} \frac{dy}{dt} = f(t, y) = \mathbf{a}(t, y)y + \mathbf{b}(t, y), & t \in (0, T], \\ y(0) = y^0. \end{cases}$$

Extension to systems in the form (1.1) is straightforward and will be discussed later on.

Given a generic non-linear ordinary differential equation, there are clearly many different ways of recasting it in the form (2.1). In applications, the identification of \mathbf{a} and \mathbf{b} is determined by the problem at hand; see (1.1). A particular class of problems for which a specific choice of the coefficients \mathbf{a} and \mathbf{b} leads to good positivity properties is analyzed in Section 3.4.

¹“An exponential integrator is a numerical method which involves an exponential function (or a related function) of the Jacobian or an approximation of it.”

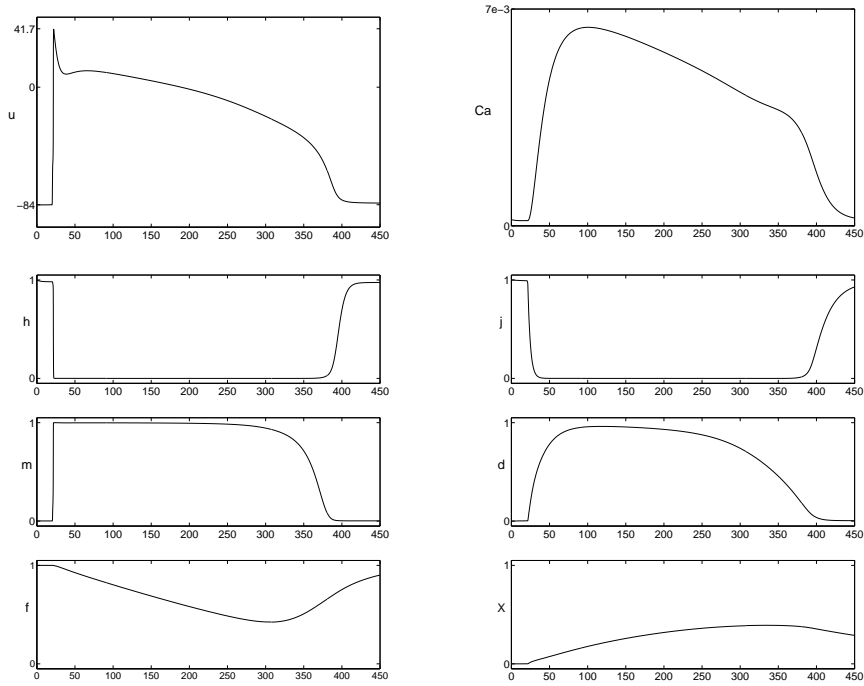


FIG. 1.1. Variables of the Luo-Rudy model as functions of time (in ms): transmembrane potential u (mV) and intracellular calcium Ca (M) in the first row, the gating variables h , j , m , d , f , and x in the last three rows.

Rush and Larsen [25] proposed the following numerical scheme for the solution of (2.1),

$$(2.2) \quad \begin{cases} y^{n+1} = e^{a^n h} \left(y^n + \frac{b^n}{a^n} \right) - \frac{b^n}{a^n}, & n = 0, \dots, N, \\ y(0) = y^0, \end{cases}$$

where y^n is the approximation of the solution $y(t^n)$, $t^n = n h$, $T = N h$, and $h > 0$ is the time-step. The expressions a^n and b^n are defined as $a^n = a(t^n, y^n)$ and $b^n = b(t^n, y^n)$, respectively. This method stems from considering the functions a and b constant on the interval $(t^n, t^{n+1}]$ and equal to a^n and b^n ; y^{n+1} is the exact solution at time t^{n+1} of the linearized differential system,

$$(2.3) \quad \begin{cases} \frac{d\tilde{y}}{dt} = a^n \tilde{y} + b^n, & t \in (t^n, t^{n+1}], \\ \tilde{y}(t^n) = y^n, \end{cases}$$

for $n = 0, \dots, N$. Even if this scheme is explicit, the stability bound is significantly less restrictive than the one of the classical Forward Euler (FE) method. For instance, when solving the Luo-Rudy model in the cases presented in Section 4, FE is stable under the condition $h \leq 0.01$ ms, while Rush-Larsen is stable for $h \leq 0.1$ ms. Moreover, the numerical solution for the gating variables is in the physiological range $[0, 1]$ with the Rush Larsen scheme even for large values of h , while this is not the case for the FE solution. We give an explanation of these results in Sections 3.3 and 3.4. Unfortunately, the original Rush-Larsen scheme is only first order accurate. We therefore devise a second order extension. Let us start by rewriting

scheme (2.2) in the following form,

$$(2.4) \quad \begin{cases} y^{n+1} = e^{a^n h} y^n + h\Phi(a^n h)b^n = y^n + h\Phi(a^n h)(a^n y^n + b^n), \\ y(0) = y^0, \end{cases}$$

for $n = 0, \dots, N$, with

$$\Phi(x) = \begin{cases} \frac{e^x - 1}{x}, & x \neq 0, \\ 1, & x = 0. \end{cases}$$

For $a = 0$ the scheme reduces to the Forward Euler (FE) scheme.

In order to increase the accuracy of this scheme, we evaluate the functions a and b at $t^{n+\frac{1}{2}}$, namely,

$$(2.5) \quad \begin{cases} y^{n+1} = y^n + h\Phi(a^{n+\frac{1}{2}}h)(a^{n+\frac{1}{2}}y^n + b^{n+\frac{1}{2}}), & n = 0, \dots, N, \\ y(0) = y^0, \end{cases}$$

where $a^{n+\frac{1}{2}}$ and $b^{n+\frac{1}{2}}$ are approximations of $a(t^{n+\frac{1}{2}})$ and $b(t^{n+\frac{1}{2}})$. In particular, we select for $n = 1, \dots, N$,

$$(2.6) \quad \begin{aligned} a^{n+\frac{1}{2}} &= c_{-1}a^{n+1} + c_0a^n + c_1a^{n-1}, & b^{n+\frac{1}{2}} &= c_{-1}b^{n+1} + c_0b^n + c_1b^{n-1}, \\ a^{\frac{1}{2}} &= c_{-1}a^1 + (c_0 + c_1)a^0, & b^{\frac{1}{2}} &= c_{-1}b^1 + (c_0 + c_1)b^0, \end{aligned}$$

where c_{-1} , c_0 , and c_1 are coefficients to be determined. For the sake of notation, in the sequel we set $\omega = c_{-1} - c_1$ and $\theta = c_{-1} + c_1$. By requiring that the approximations (2.6) are exact for both constant and linear functions, we get the constraints

$$(2.7) \quad \left. \begin{aligned} c_{-1} + c_0 + c_1 = \theta + c_0 = 1 \\ c_{-1} - c_1 = \omega = \frac{1}{2} \end{aligned} \right\} \Rightarrow c_{-1} = \frac{\theta}{2} + \frac{1}{4}, \quad c_0 = 1 - \theta, \quad \text{and } c_1 = \frac{\theta}{2} - \frac{1}{4}.$$

We can force (2.6) to be exact also for quadratic functions (yielding third order accuracy of the approximation (2.6)) with $c_0 = 3/4$, $c_1 = 3/8$ and $c_{-1} = -1/8$. However, this does not improve the overall accuracy of the scheme, as we prove in the next subsection (see (3.2) below), since this just improves the accuracy in the estimates of $a^{n+\frac{1}{2}}$ and $b^{n+\frac{1}{2}}$, not the accuracy of the linearization procedure in (2.5). Therefore, we select θ on the basis of stability or efficiency constraints rather than on accuracy arguments.

3. Analysis of the methods.

3.1. Consistency. If a and b are sufficiently regular functions, the following local truncation error (LTE) can be derived from standard Taylor expansions (prime symbol means differentiation),

$$(3.1) \quad (\text{LTE}_1) = \frac{1}{h}(y(t^{n+1}) - y^{n+1}) = \left(\frac{1}{2} - \omega\right) (a'(t^n)y(t^n) - b'(t^n))h + o(h).$$

In particular, for $\omega = \frac{1}{2}$, the first term on the right hand side vanishes. Upon expanding the $o(h)$ term, the local truncation error reads

$$(3.2) \quad (\text{LTE}_2) = \left(\frac{1}{6} - \frac{\theta}{2}\right) (a''(t^n)y_i(t^n) - b''(t^n))h^2 + \frac{1}{12}(a'(t^n)b^n - a^n b'(t^n))h^2 + o(h^2).$$

TABLE 3.1
Coefficients of the numerical schemes.

| | c_{-1} | c_0 | c_1 |
|----------------------|----------------------------------|----------------|----------------------------------|
| FE* | 0 | 1 | 0 |
| $M^*(\theta)$ | $\frac{\theta}{2} + \frac{1}{4}$ | $1 - \theta$ | $\frac{\theta}{2} - \frac{1}{4}$ |
| AB2* ($M^*(-1/2)$) | 0 | $\frac{3}{2}$ | $-\frac{1}{2}$ |
| CN* ($M^*(1/2)$) | $\frac{1}{2}$ | $\frac{1}{2}$ | 0 |
| AM3* ($M^*(1/3)$) | $\frac{5}{12}$ | $\frac{8}{12}$ | $-\frac{1}{12}$ |

From (3.1) and (3.2), we get that the LTE vanishes when $h \rightarrow 0$ (consistency). However, the dependence of LTE on h is at most quadratic, independently of θ , due to the presence of the boxed term. This limits the accuracy of the schemes (2.5) to second order.

Notice that the proposed schemes reduce to classical two-step Adams schemes when $a = 0$. As a matter of fact, in this case the scheme reduces to

$$y^{n+1} = y^n + h \left(\left(\frac{\theta}{2} + \frac{1}{4} \right) b^{n+1} + (1 - \theta) b^n + \left(\frac{\theta}{2} - \frac{1}{4} \right) b^{n-1} \right), \quad n = 0, \dots, N.$$

We denote these schemes $M(\theta)$ and their generalization to the case $a \neq 0$ is indicated with $M^*(\theta)$. Observe, in particular, that $M(-\frac{1}{2})$, $M(\frac{1}{2})$, and $M(\frac{1}{3})$ correspond to the classical Adams-Bashforth two-step scheme (hereafter denoted by AB2), the Crank-Nicolson scheme (CN), and the Adams-Moulton two-step scheme (AM3), respectively. By extension, we will denote by AB2*, CN*, and AM3* the methods $M^*(-\frac{1}{2})$, $M^*(\frac{1}{2})$, $M^*(\frac{1}{3})$, respectively. We also use the short notation FE* for the Rush-Larsen scheme ($c_{-1} = 0$, $c_0 = 1$, and $c_1 = 0$). In Table 3.1 we report the coefficients for the numerical schemes used in this paper.

REMARK 3.1. When a is constant, our schemes can be regarded in the class of Exponential Time Differencing (ETD) methods [2, 18] or in the class of exponential multistep methods [2, 19, 20]. These methods have been devised for semi-linear problems of the form

$$\frac{\partial y}{\partial t} = Ly + N(y), \quad y(0) = y_0.$$

However, even if the Rush-Larsen FE* actually corresponds to the first order exponential Adam Bashforth scheme, the linearization underlying the $M^*(\theta)$ schemes presented here makes them different from the schemes mentioned in the cited papers (and of course from other classical methods) and deserve therefore a specific analysis.

3.2. Stability and convergence. We give first a definition of zero-stability adapted to our scheme.

DEFINITION 3.2. A numerical method in the form (2.5) is zero-stable when

$$\exists h_0 > 0, \exists C > 0 : \forall h \in (0, h_0], \quad |z^n - y^n| \leq C\varepsilon, \quad 0 \leq n \leq N,$$

where y^n is the solution to problem (2.5) and z^n is the solution of the perturbed problem

$$(3.3) \quad \begin{cases} z^{n+1} = z^n + h\Phi(ah) [a^{n+\frac{1}{2}} z^n + b^{n+\frac{1}{2}}] + h\delta^{n+1}, \\ z^0 = y^0 + \delta^0, \end{cases}$$

for $0 \leq n \leq N - 1$, under the assumption that $|\delta^k| \leq \varepsilon$, $0 \leq k \leq N - 1$.

PROPOSITION 3.3. *The scheme (2.5) is zero-stable under the following conditions:*

- i) *a and b are Lipschitz continuous functions with respect to the second argument (y) and uniformly with respect to t, with constants L_a and L_b , respectively.*
- ii) *There exists a non-negative constant a_M such that*

$$(3.4) \quad a(t, y) \leq a_M, \quad \forall y \in \mathbb{R}^m, t \in [0, T].$$

It is worth noting that in gating variable models (1.1) typically $a_i < 0$; hence, condition (ii) holds. This is true, in particular, for the Luo-Rudy model. Before proving Proposition 3.3, we state the following Lemma.

LEMMA 3.4. *Let x^n satisfy*

$$(3.5) \quad 0 \leq x^n \leq \xi x^{n-1} + \eta x^{n-2} + (\xi + \eta - 1)\delta,$$

where $\eta \geq 0$, $\delta \geq 0$, $x^0, x^1 \geq 0$, and $\xi \geq 1$ are given data. Then,

$$x^n \leq \left[x^0 + \delta + \frac{2}{\xi}(x^1 + \delta) \right] (\xi + \eta)^n.$$

Proof. Consider the difference equation

$$(3.6) \quad \tilde{x}^n = \xi \tilde{x}^{n-1} + \eta \tilde{x}^{n-2} + (\xi + \eta - 1)\delta,$$

with $\tilde{x}^0 = x^0$ and $\tilde{x}^1 = x^1$. We have obviously that $x^n \leq \tilde{x}^n$. Observe that under the given assumptions the right-hand side is non-negative, so that $\tilde{x}^n \geq 0$, which is compatible with the first inequality in (3.5). The solution to the difference equation (3.6) is

$$\tilde{x}^n = \sigma_1 \rho_1^n + \sigma_2 \rho_2^n - \delta,$$

with

$$\rho_{1,2} = \frac{1}{2} \left(\xi \pm \sqrt{\xi^2 + 4\eta} \right), \quad \sigma_1 = \frac{(x^1 + \delta) - \rho_2(x^0 + \delta)}{\rho_1 - \rho_2}, \quad \text{and} \quad \sigma_2 = \frac{\rho_1(x^0 + \delta) - (x^1 + \delta)}{\rho_1 - \rho_2}.$$

It can be verified that $|\rho_{1,2}| \leq \xi + \eta$, $\rho_1 - \rho_2 \geq \xi$, and $\sigma_1 > 0$, so that

$$x^n \leq \tilde{x}^n \leq \sigma_1 \rho_1^n + |\sigma_2| |\rho_2|^n \leq (\sigma_1 + |\sigma_2|) (\xi + \eta)^n.$$

The lemma thus follows after some algebra exploiting the fact that $x^1 + \delta \geq 0$, $x^0 + \delta \geq 0$, and $\rho_1 - \rho_2 \geq \xi$. \square

Proof of Proposition 3.3. Let us rewrite (2.5) as

$$(3.7) \quad y^{n+1} = e^{a^{n+\frac{1}{2}}h} y^n + \Phi(a^{n+\frac{1}{2}}h) b^{n+\frac{1}{2}}, \quad n = 0, \dots, N.$$

For $a \leq a_M$, $\tilde{a} \leq a_M$, and $h \in (0, h_0]$, we have

$$(3.8) \quad \begin{aligned} |\Phi(a h)| &\leq \Phi_M, & |\Phi(a h) - \Phi(\tilde{a} h)| &\leq h L_\Phi |a - \tilde{a}|, \\ |e^{a h}| &\leq e^{a_M h}, & |e^{a h} - e^{\tilde{a} h}| &\leq h L_e |a - \tilde{a}|, \end{aligned}$$

where $\Phi_M = \Phi(a_M h_0)$, $L_\Phi = \Phi'(a_M h_0)$, and $L_e = e^{a_M h_0}$.

For the sake of notation, let us write a_y^n and b_y^n in place of $a(t^n, y^n)$ and $b(t^n, y^n)$, respectively, and a_z^n and b_z^n for $a(t^n, z^n)$ and $b(t^n, z^n)$. First, we prove that y^n and b_y^n are bounded for all $n = 1, \dots, N$. From equation (3.7), we have

$$(3.9) \quad |y^n| \leq e^{a_M h} |y^{n-1}| + h \Phi_M |b_y^{n-\frac{1}{2}}|, \quad n = 2, \dots, N.$$

Notice that $|\mathfrak{b}(y, t)| \leq B_0 + L_b|y|$ for all $t \in [0, T]$, where $B_0 = \max_{t \in [0, T]} |\mathfrak{b}(t, 0)|$. Hence, we can write

(3.10)

$$|\mathfrak{b}_y^{n-\frac{1}{2}}| \leq \sum_{k=-1}^1 |c_k \mathfrak{b}_y^{n-k-1}| \leq \sum_{k=-1}^1 |c_k B_0| + L_b \sum_{k=-1}^1 |c_k| |y^{n-k-1}|, \quad n = 2, \dots, N.$$

Substituting (3.10) into (3.9), we have

$$(3.11) \quad \alpha |y^n| \leq \beta |y^{n-1}| + \gamma |y^{n-2}| + hc \Phi_M B_0, \quad n = 2, \dots, N,$$

where $\alpha = 1 - h|c_{-1}|L_b\Phi_M$, $\beta = e^{h a_M} + h|c_0|L_b\Phi_M$, $\gamma = h|c_1|L_b\Phi_M$ and $c = |c_{-1}| + |c_0| + |c_1|$. Taking h_0 such that $\alpha > 0 \quad \forall h \in (0, h_0]$, we can apply Lemma 3.4 and obtain, for $n = 2, \dots, N$,

$$|y^n| \leq \left(|y^0| + 2\frac{\alpha}{\beta}|y^1| + \left(1 + 2\frac{\alpha}{\beta}\right) \frac{hc\Phi_M B_0 \alpha}{e^{h a_M} - 1 + hc\Phi_M L_b} \right) \times \left(\frac{e^{h a_M} + h(|c_0| + |c_1|)L_b\Phi_M}{1 - h|c_{-1}|L_b\Phi_M} \right)^n.$$

Since $\alpha \leq 1$ and $e^{h a_M} - 1 > 0$, we can write

$$\begin{aligned} |y^n| &\leq K_1 \left(\frac{e^{h a_M} + h(|c_0| + |c_1|)L_b\Phi_M}{1 - h|c_{-1}|L_b\Phi_M} \right)^n \\ &= K_1 e^{a_M n h} \left(1 + \frac{h|c_{-1}|L_b\Phi_M}{1 - h|c_{-1}|L_b\Phi_M} \right)^n \left(1 + h(|c_0| + |c_1|) \frac{L_b\Phi_M}{e^{a_M h}} \right)^n, \end{aligned}$$

with $K_1 = \left(|y^0| + 2\frac{\alpha}{\beta}|y^1| + \left(1 + 2\frac{\alpha}{\beta}\right) \frac{B_0}{L_b} \right)$. Exploiting the well-known inequality $(1+x)^n \leq e^{nx}$ for $x \geq 0$, we have

$$|y^n| \leq K_1 e^{a_M T} e^{(|c_{-1}|(1-h_0|c_{-1}|L_b\Phi_M)^{-1} + |c_0| + |c_1|)L_b\Phi_M T} = y_M.$$

Since $\alpha |y^1| \leq (\beta + \gamma)|y^0| + c h_0 \Phi_M B_0$, we conclude that y^n is bounded. Also \mathfrak{b}_y^n is bounded $\forall n \in [0, N]$ since $|\mathfrak{b}_y^n| \leq B_0 + L_b y_M = b_M$. Setting $w^n = z^n - y^n$ and subtracting (3.3) from (2.5), we obtain

$$(3.12) \quad w^n = h\delta^n + e^{h a_z^{n-\frac{1}{2}}} z^{n-1} - e^{h a_y^{n-\frac{1}{2}}} y^{n-1} + h\Phi(h a_z^{n-\frac{1}{2}}) \mathfrak{b}_z^{n-\frac{1}{2}} - h\Phi(h a_y^{n-\frac{1}{2}}) \mathfrak{b}_y^{n-\frac{1}{2}},$$

for $n = 1, \dots, N$. Let us analyze separately the terms of the previous equation,

$$\begin{aligned} &\left| e^{h a_z^{n-\frac{1}{2}}} z^{n-1} - e^{h a_y^{n-\frac{1}{2}}} y^{n-1} \right| \\ &= \left| e^{h a_z^{n-\frac{1}{2}}} w^{n-1} + \left(e^{h a_z^{n-\frac{1}{2}}} - e^{h a_y^{n-\frac{1}{2}}} \right) y^{n-1} \right| \\ &\leq e^{h a_M} |w^{n-1}| + h y_M L_e \left| a_z^{n-\frac{1}{2}} - a_y^{n-\frac{1}{2}} \right| \\ &\leq e^{h a_M} |w^{n-1}| + h y_M L_e L_a \left(\sum_{i=-1}^1 |c_i| |w^{n-i-1}| \right), \end{aligned}$$

$$\begin{aligned} &\left| \Phi(h a_z^{n-\frac{1}{2}}) \mathfrak{b}_z^{n-\frac{1}{2}} - \Phi(h a_y^{n-\frac{1}{2}}) \mathfrak{b}_y^{n-\frac{1}{2}} \right| \\ &= \left| \Phi(h a_z^{n-\frac{1}{2}}) (\mathfrak{b}_z^{n-\frac{1}{2}} - \mathfrak{b}_y^{n-\frac{1}{2}}) + (\Phi(h a_z^{n-\frac{1}{2}}) - \Phi(h a_y^{n-\frac{1}{2}})) \mathfrak{b}_y^{n-\frac{1}{2}} \right| \\ &\leq \Phi_M \left| \mathfrak{b}_z^{n-\frac{1}{2}} - \mathfrak{b}_y^{n-\frac{1}{2}} \right| + b_M L_\Phi \left| a_z^{n-\frac{1}{2}} - a_y^{n-\frac{1}{2}} \right| \\ &\leq (\Phi_M L_b + h b_M L_\Phi L_a) \left(\sum_{i=-1}^1 |c_i| |w^{n-i-1}| \right). \end{aligned}$$

From equation (3.12), using the previous inequalities, we obtain

$$\alpha|w^n| \leq \beta|w^{n-1}| + \gamma|w^{n-2}| + h\varepsilon,$$

where $\alpha = 1 - h|c_{-1}|K_2$, $\beta = e^{h a_M} + h|c_0|K_2$, $\gamma = h|c_1|K_2$ with $K_2 = (y_M L_e L_a + \Phi_M L_b + h_0 b_m L_\Phi L_a)$. Again, for h_0 such that $\alpha > 0 \forall h \in (0, h_0]$, we can apply Lemma 3.4 and obtain

$$|w^n| \leq \left(|w^0| + 2\frac{\alpha}{\beta}|w^1| + \left(1 + 2\frac{\alpha}{\beta}\right) \frac{\varepsilon}{cK_2} \right) \left(\frac{e^{h a_M} + h(|c_0| + |c_1|)K_2}{1 - h|c_{-1}|K_2} \right)^n,$$

for $n = 2, \dots, N$. Noticing that $|w^0| \leq \varepsilon$, $\alpha|w^1| \leq (\beta + \gamma)|w^0| + h_0\varepsilon$ and that $(1+x)^n \leq e^{nx}$ for $x \geq 0$, we obtain, for $n = 1, \dots, N$,

$$\begin{aligned} |w^n| &\leq \varepsilon \left(3 + 2\frac{\gamma}{\beta} + \frac{\beta + 2\alpha}{\beta cK_2} \right) \left(1 + \frac{h|c_{-1}|K_2}{1 - h|c_{-1}|K_2} \right)^n e^{a_M n h} e^{(|c_0| + |c_1|)K_2 n h} \\ &\leq \varepsilon \left(3 + 2\frac{\gamma}{\beta} + \frac{\beta + 2\alpha}{\beta cK_2} \right) e^{a_M T} e^{(|c_{-1}|(1-h_0|c_{-1}|C)^{-1} + |c_0| + |c_1|)CT}, \end{aligned}$$

which proves the proposition. This argument can be easily extended to the vector case when the exponential matrices associated with the scheme are diagonal, which is actually our case. In this circumstance, the expressions have to be interpreted component-wise, and the absolute value ($|\cdot|$) has to be replaced by the infinite norm for both vectors and matrices ($\|\cdot\|_\infty$). \square

If $a(t, y)$ and $b(t, y)$ are sufficiently regular functions, from zero-stability and consistency, we can prove that the method is convergent of order 2, if $\omega = 1/2$, and of order 1, otherwise.

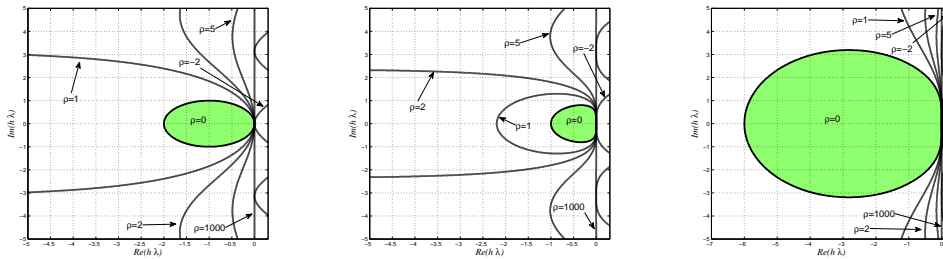


FIG. 3.1. Absolute stability regions for the FE* (left), the AB2* (center) and AM3* methods when applied to the model problem $y' = \lambda y$ with $\lambda = \lambda_a + \lambda_b$, $a = \lambda_a$, $b = \lambda_b y$ and $\lambda_a = \rho \lambda_b$ with ρ a real parameter.

3.3. Absolute stability. The stability over long time intervals for the linear model problem $y = \lambda y$, with $Re(\lambda) < 0$, strongly depends on the implementation of the method, i.e., on the definition of a and b with respect to the model problem. In particular, since the part determined by a is solved exactly for the model problem, if we set $a = \lambda$ ($b = 0$), we get an unconditionally stable method, while for $a = 0$ and $b = \lambda y$ stability of the method is the same as for the corresponding multistep method. These preliminary observations agree with the experimental results mentioned above concerning the FE* method, which is more stable than the corresponding FE scheme. In order to be more quantitative, we split $\lambda = \lambda_a + \lambda_b$ and consider the (scalar) scheme (2.5) with $a = \lambda_a$ and $b = \lambda_b$. In particular, we write $\lambda_a = \rho \lambda_b$, where ρ is a non-negative parameter, and investigate the time asymptotic solution

dynamics for different values of ρ and different schemes. A similar approach for the analysis of absolute stability has been used in [2, 15]. We report here the results for the sake of completeness.

By standard arguments on finite difference equations, we obtain that the solution computed by our scheme asymptotically vanishes if the roots of the polynomial

$$\left(1 - \frac{e^{\frac{\rho\lambda h}{\rho+1}} - 1}{\rho} c_{-1}\right) r^2 - \left(1 + \left(e^{\frac{\rho\lambda h}{\rho+1}} - 1\right) \left(1 + \frac{c_0}{\rho}\right)\right) r - c_1 \frac{e^{\frac{\rho\lambda h}{\rho+1}} - 1}{\rho} = 0$$

are strictly inside the unit circle in the complex plane. We stress that for $\rho \rightarrow 0$ we recover the characteristic polynomial of the method $M(\theta)$. In Figure 3.1 we report the region of absolute stability of FE^* , $AB2^*$, and $AM3^*$, respectively. The shaded region is the region of absolute stability of the corresponding traditional multistep method. As expected, when ρ gets larger the region of absolute stability increases and the method at hand tends to become unconditionally stable (and exact for the model problem).

This analysis gives an interesting perspective on the methods addressed here, which can be considered a sort of “stabilization” of traditional schemes, obtained by limiting the accuracy to the second order.

Observe that for $\rho < -1$ and $\lambda < 0$, we have $\lambda_a < 0$ and $\lambda_b > 0$, which is the situation we have from the linearization of problems coming from electro-physiology. In this case, the region of absolute stability covers the entire half plane.

3.4. Positivity properties. As pointed out previously, one of the interesting features of the Rush-Larsen scheme when applied to the gating equations, is that the numerical solution is guaranteed to belong to the interval $[0, 1]$. Here, we investigate the positivity properties of our schemes, giving a rigorous proof that holds also for the Rush-Larsen scheme itself. For the sake of simplicity we consider the scalar case. The extension to the vector case, for diagonal exponential matrices, can be carried out component-wise. Let us start with some assumptions on the continuous problems, which are, in particular, satisfied for the applications of interest here.

Let us suppose that there exist a function $a(t, y) < 0$ and constants K_1, K_2 , such that

$$(3.13) \quad a(t, y)(y - K_1) \leq f(t, y) \leq a(t, y)(y - K_2), \quad \forall y \in \mathbb{R}, t \in (0, T].$$

Then $y \in [K_1, K_2]$ provided that $y^0 \in [K_1, K_2]$ (in the case of gating variables $K_1 = 0$ and $K_2 = 1$). This can be proved considering the subsolution \underline{y} and the supersolution \overline{y} , which satisfy the equations,

$$(3.14) \quad \begin{cases} \frac{d\underline{y}}{dt} = a(t, \underline{y})(\underline{y} - K_1) \\ \underline{y}(0) = y_0 \end{cases} \quad \begin{cases} \frac{d\overline{y}}{dt} = a(t, \overline{y})(\overline{y} - K_2) \\ \overline{y}(0) = y_0. \end{cases}$$

We have that $\underline{y} \leq y \leq \overline{y}$. We claim that $\underline{y} \geq K_1$. In fact, multiplying the first equation in (3.14) by $(\underline{y} - K_1)$, we get

$$\frac{1}{2} \frac{d}{dt} (\underline{y} - K_1)^2 = a(t, \underline{y})(\underline{y} - K_1)^2 \leq 0.$$

Hence, since $(\underline{y} - K_1)^2$ is non-increasing in time, if there exists $\tau \in [0, T]$ such that $\underline{y}(\tau) = K_1$, then $\underline{y}(t) = K_1$ for all $t \in [\tau, T]$. With same arguments we conclude that $\overline{y}(t) \leq K_2$. Hence $K_1 \leq \underline{y} \leq y \leq \overline{y} \leq K_2$.

PROPOSITION 3.5. *Under the assumption (3.13), the scheme (2.5) with non-negative coefficients c_{-1} , c_0 and c_1 , has a numerical solution $y^n \in [K_1, K_2]$, provided that $y^0 \in [K_1, K_2]$.*

Proof. Let $b(t, y) = f(t, y) - a(t, y)y$. Application of our scheme yields

$$y^{n+1} = e^{a^{n+\frac{1}{2}}h}y^n + \left(1 - e^{a^{n+\frac{1}{2}}h}\right) \left(-\frac{b^{n+\frac{1}{2}}}{a^{n+\frac{1}{2}}}\right).$$

We start assuming that $a^{n+\frac{1}{2}}$ and $b^{n+\frac{1}{2}}$ do coincide exactly with $a(t^{n+\frac{1}{2}})$ and $b(t^{n+\frac{1}{2}})$. Observe that from our assumptions $K_1 \leq b^{n+\frac{1}{2}}/a^{n+\frac{1}{2}} \leq K_2$. Under the assumption (3.13), if $y^n \in [K_1, K_2]$, then y^{n+1} is the convex combination (with coefficients $e^{a^{n+\frac{1}{2}}h}$ and $1 - e^{a^{n+\frac{1}{2}}h}$) of terms belonging to the range $[K_1, K_2]$. Hence, y^{n+1} belongs to the same range. By induction, we conclude that y^n belongs to $[K_1, K_2]$ when y^0 does.

Now, we have to investigate the impact of the approximations $a^{n+\frac{1}{2}} \simeq a(t^{n+\frac{1}{2}})$ and $b^{n+\frac{1}{2}} \simeq b(t^{n+\frac{1}{2}})$ on this statement. If the three coefficients c_{-1}, c_0, c_1 are nonnegative, then the combination still has positive coefficients and $-\frac{b^{n+\frac{1}{2}}}{a^{n+\frac{1}{2}}}$ is in the range $[K_1, K_2]$. \square

Notice that the latter proposition includes the schemes FE*, CN*, and M(θ)* with $\theta > 0$. In particular, this proposition does not include scheme AB2*. We specifically analyse AB2* in the next proposition.

PROPOSITION 3.6. *Let $f(t, y)$ satisfy the inequalities (3.13) with a constant, $y^0 \in [K^1, K^2]$. Then the scheme AB2* is such that the numerical solution y^n belongs to $[K^1, K^2]$ under the condition*

$$(3.15) \quad h \leq \frac{\log(2)}{|a|}.$$

Moreover, if the initial conditions are such that

$$(3.16) \quad \left(\frac{3}{2}e^{ah} - \frac{1}{2}\right) K_1 \leq e^{ah}y^1 - h\Phi\left(\frac{1}{2}\right)b^0 \leq \left(\frac{3}{2}e^{ah} - \frac{1}{2}\right) K_2,$$

the restriction on h can be relaxed to

$$(3.17) \quad h \leq \frac{\log(3)}{|a|}.$$

Proof. Notice that when y^n fulfills (2), then $u^n := y^n - K^1$ satisfies the scheme $u^{n+1} = u^n + h\Phi(ah)(au^n + \tilde{b}^{n+\frac{1}{2}})$, where $\tilde{b}^{n+\frac{1}{2}} := \frac{3}{2}\tilde{b}^n - \frac{1}{2}\tilde{b}^{n-1}$ and $\tilde{b}^n := b^n + aK^1$. In fact,

$$(3.18) \quad \begin{aligned} u^{n+1} &= y^{n+1} - K^1 = y^n + h\Phi(ah) \left(ay^n + b^{n+\frac{1}{2}}\right) - K^1 \\ &= y^n - K^1 + h\Phi(ah) \left(a(y^n - K^1) + (b^{n+\frac{1}{2}} + aK^1)\right) \\ &= u^n + h\Phi(ah) \left(au^n + \tilde{b}^{n+\frac{1}{2}}\right). \end{aligned}$$

Moreover (3.13) implies $\tilde{b}^n \geq 0$. Analogously, $u^n := K^2 - y^n$ satisfies the same scheme, with $\tilde{b}^n := -b^n - aK^2$ and $\tilde{b}^n \geq 0$; hence, by proving that $u^n \geq 0$, we prove that $y^n \in [K^1, K^2]$. We prove that $u^n \geq 0$ by induction. Let us define $s^n = e^{ah}u^n - h\Phi(ah)\frac{1}{2}\tilde{b}^{n-1}$. We have

1. $s^1 \geq 0$. More precisely,

$$s^1 = e^{ah}u^1 - h\Phi(ah)\frac{1}{2}\tilde{b}^0,$$

which is nonnegative when (3.16) holds; otherwise, since $u^1 = e^{ah}u^0 + h\Phi(ah)\tilde{b}^0$, s^1 can be written as

$$s^1 = e^{2ah}u^0 + h\Phi(ah)\left(e^{ah} - \frac{1}{2}\right)\tilde{b}^0,$$

which is nonnegative when $\left(e^{ah} - \frac{1}{2}\right) \geq 0$, i.e., when (3.15) holds.

2. $s^n \geq 0 \implies s^{n+1} \geq 0$, $n = 1, \dots, N-1$.

In fact, $u^{n+1} = e^{ah}u^n + h\Phi(ah)\left(\frac{3}{2}\tilde{b}^n - \frac{1}{2}\tilde{b}^{n-1}\right)$. Hence

$$\begin{aligned} (3.19) \quad s^{n+1} &= e^{ah}u^{n+1} - h\Phi(ah)\frac{1}{2}\tilde{b}^n \\ &= e^{ah}\left[e^{ah}u^n + h\Phi(ah)\left(\frac{3}{2}\tilde{b}^n - \frac{1}{2}\tilde{b}^{n-1}\right)\right] - h\Phi(ah)\frac{1}{2}\tilde{b}^n \\ &= e^{ah}\left[e^{ah}u^n - h\Phi(ah)\frac{1}{2}\tilde{b}^{n-1}\right] + h\Phi(ah)\left(\frac{3}{2}e^{ah} - \frac{1}{2}\right)\tilde{b}^n \\ &\geq e^{ah}s^n + h\Phi(ah)\left(\frac{3}{2}e^{ah} - \frac{1}{2}\right)\tilde{b}^n \geq h\Phi(ah)\left(\frac{3}{2}e^{ah} - \frac{1}{2}\right)\tilde{b}^n. \end{aligned}$$

The last term is nonnegative when $\left(\frac{3}{2}e^{ah} - \frac{1}{2}\right) \geq 0$, i.e., when (3.17) holds (notice that $s^n \geq 0 \implies u^n \geq 0$, since $e^{ah}u^n \geq +h\Phi(ah)\frac{1}{2}\tilde{b}^{n-1} \geq 0$; for this reason $\tilde{b}^n \geq 0$).

Hence, by induction, $s^n \geq 0$, $n = 1, \dots, N$. This implies $u^n \geq 0$. \square

Restrictions on h (3.15) and (3.17) are to be compared with those of AB2 [12], namely, $h \leq \frac{1}{3|a|}$ and $h \leq \frac{4}{9|a|}$ respectively. Positivity bounds on h for AB2* are significantly less restrictive than those for AB2.

4. The scheme at work. In this section we show how to use the proposed scheme for the solution of system (1.1). We consider the vector form of scheme (2.5),

$$(4.1) \quad \begin{cases} y_i^{n+1} = y_i^n + h\Phi(a_i^{n+\frac{1}{2}}h)(a_i^{n+\frac{1}{2}}y_i^n + b_i^{n+\frac{1}{2}}), & n = 0, \dots, N, i = 1, \dots, m, \\ \mathbf{y}(0) = \mathbf{y}^0, \end{cases}$$

where vectors with entries a_i and b_i are denoted by \mathbf{a} and \mathbf{b} . We take $\mathbf{a} = [0, \mathbf{a}^T, \mathbf{0}^T]^T$ and $\mathbf{b} = [I, \mathbf{b}^T, \mathbf{g}^T]^T$. Hence, the scheme (4.1) reads as follows,

$$(4.2) \quad \begin{cases} \frac{1}{h}u^{n+1} = \frac{1}{h}u^n + c_{-1}I^{n+1} + c_0I^n + c_1I^{n-1}, \\ \frac{1}{h}w_i^{n+1} = \frac{1}{h}w_i^n + \Phi(a_i^{n+\frac{1}{2}}h)\left(a_i^{n+\frac{1}{2}}w_i^n + b_i^{n+\frac{1}{2}}\right), & i = 1, \dots, m, \\ \frac{1}{h}\mathbf{X}^{n+1} = \frac{1}{h}\mathbf{X}^n + c_{-1}\mathbf{g}^{n+1} + c_0\mathbf{g}^n + c_1\mathbf{g}^{n-1}, \\ u(0) = u_0, \quad \mathbf{w}(0) = \mathbf{w}_0, \quad \mathbf{X}(0) = \mathbf{X}_0, \end{cases}$$

for $n = 0, \dots, N$. We take $I^{-1} = I^0$ and $\mathbf{g}^{-1} = \mathbf{g}^0$. The following results are obtained using the Luo-Rudy phase I model with the following current stimulus,

$$(4.3) \quad I_{app} = \begin{cases} I_{max}\left(\frac{1}{2} - \frac{1}{2}\cos\left(2\pi\frac{t}{t_p}\right)\right), & t < t_p, \\ 0, & t \geq t_p, \end{cases} \quad I_{max} = 60\mu A, \quad t_p = 1ms,$$

and $C_m = 1\mu F$. We refer to the discrete L^2 norm of the components of solution y^n , defined by

$$\|y_i\| = \sqrt{\frac{1}{2} \sum_{n=0}^{N-1} \left[(y_i^n)^2 + (y_i^{n+1})^2 \right] (t^{n+1} - t^n)}.$$

The relative error is computed as $\max_i \frac{\|y_i(t^n) - y_i^n\|}{\|y_i(t^n)\|}$. In the following simulations, we will take $T = 450 \text{ ms}$. In Table 4.1 we compare the relative errors for different time-steps using our explicit method AB2*, FE*, and their corresponding multistep methods, AB2 and FE. The “reference” solution, i.e., the solution used as the exact one, is obtained by solving the system with the Matlab function `ode45` with parameters `RelTol` and `AbsTol` set respectively to $1e - 9$ and $1e - 12$. Results confirm that the AB2* method is second order accurate versus the first order accuracy of the Rush-Larsen method. Observe that for tiny time-steps multistep methods feature slightly better accuracy than the corresponding starred methods. However, their stability constraints are more restrictive, requiring $h \simeq 0.01 \text{ ms}$.

TABLE 4.1
Relative error using different time-steps and the methods AB2, FE*, AB2, and FE.*

| h | err_{rel} AB2* | err_{rel} FE* | err_{rel} AB2 | err_{rel} FE |
|---------|------------------|-----------------|-----------------|----------------|
| 2e-1 | 1.03e-1 | 1.02e-1 | NaN | NaN |
| 1e-1 | 8.73e-3 | 6.72e-2 | NaN | NaN |
| 5e-2 | 3.64e-3 | 3.98e-2 | NaN | NaN |
| 2.5e-2 | 1.28e-3 | 2.16e-2 | NaN | NaN |
| 1.25e-2 | 3.63e-4 | 1.12e-2 | NaN | 6.65e-3 |
| 6.25e-3 | 9.71e-5 | 5.65e-3 | 5.65e-5 | 3.33e-3 |

4.1. Predictor-corrector strategy. In this section we recast our schemes in a predictor-corrector (PC) framework; for an introduction to predictor-corrector schemes, see, e.g., [16, 24]. Let \hat{y}^n be the solution obtained with the predictor scheme (explicit), and y^n the one obtained with the corrector scheme (implicit); let \bar{c}_0 and \bar{c}_1 be the coefficients of predictor scheme ($\bar{c}_{-1} = 0$) and c_{-1}, c_0, c_1 the coefficients of the corrector scheme. The PC time discretization of system (1.1), for $n = 1, \dots, N$, reads

$$(4.4) \quad \begin{cases} P : \begin{cases} \frac{1}{h} \hat{u}^{n+1} = \frac{1}{h} u^n + \bar{c}_0 I^n + \bar{c}_1 I^{n-1}, \\ \frac{1}{h} \hat{w}_i^{n+1} = \frac{1}{h} w_i^n + \Phi(\bar{a}_i^{n+\frac{1}{2}} h) \left(\bar{a}_i^{n+\frac{1}{2}} w_i^n + \bar{b}_i^{n+\frac{1}{2}} \right), \quad i = 1, \dots, m, \\ \frac{1}{h} \hat{X}^{n+1} = \frac{1}{h} X^n + \bar{c}_0 g^n + \bar{c}_1 g^{n-1}, \end{cases} \\ C : \begin{cases} \frac{1}{h} u^{n+1} = \frac{1}{h} u^n + c_{-1} \hat{I}^{n+1} + c_0 I^n + c_1 I^{n-1}, \\ \frac{1}{h} w_i^{n+1} = \frac{1}{h} w_i^n + \Phi(\hat{a}_i^{n+\frac{1}{2}} h) \left(\hat{a}_i^{n+\frac{1}{2}} w_i^n + \hat{b}_i^{n+\frac{1}{2}} \right), \quad i = 1, \dots, m, \\ \frac{1}{h} X^{n+1} = \frac{1}{h} X^n + c_{-1} \hat{g}^{n+1} + c_0 g^n + c_1 g^{n-1}, \end{cases} \end{cases}$$

where \hat{I}^{n+1} and \hat{g}^{n+1} are computed using the predictor solutions $\hat{u}^{n+1}, \hat{w}^{n+1}, \hat{X}^{n+1}$, and

$$(4.5) \quad \begin{aligned} \bar{a}^{n+\frac{1}{2}} &= \bar{c}_0 a^n + \bar{c}_1 a^{n-1}, & \bar{b}^{n+\frac{1}{2}} &= \bar{c}_0 b^n + \bar{c}_1 b^{n-1}, \\ \hat{a}^{n+\frac{1}{2}} &= c_{-1} a(\hat{u}^{n+1}) + c_0 a^n + c_1 a^{n-1}, & \hat{b}^{n+\frac{1}{2}} &= c_{-1} b(\hat{u}^{n+1}) + c_0 b^n + c_1 b^{n-1}, \\ \bar{a}^{\frac{1}{2}} &= (\bar{c}_0 + \bar{c}_1) a^0, & \bar{b}^{\frac{1}{2}} &= (\bar{c}_0 + \bar{c}_1) b^0, \\ \hat{a}^{\frac{1}{2}} &= c_{-1} a(\hat{u}^1) + (c_0 + c_1) a^0, & \hat{b}^{\frac{1}{2}} &= c_{-1} b(\hat{u}^1) + (c_0 + c_1) b^0. \end{aligned}$$

TABLE 4.2

Relative errors using different time-steps for the predictor-corrector methods AB2*-CN*, FE*-CN*. The results in the first two columns refer to the PECE approach, the ones in last two columns to the PEC approach.

| h | AB2*-CN* | FE*-CN* | AB2*-CN* _{PEC} | FE*-CN* _{PEC} |
|---------|----------|---------|-------------------------|------------------------|
| 2e-1 | 3.41e-2 | 5.65e-2 | NaN | 4.26e-2 |
| 1e-1 | 9.02e-3 | 2.33e-2 | 1.50e-2 | 3.04e-2 |
| 5e-2 | 2.97e-3 | 7.72e-3 | 4.15e-3 | 1.26e-2 |
| 2.5e-2 | 6.95e-4 | 2.23e-3 | 9.00e-4 | 3.95e-3 |
| 1.25e-2 | 1.57e-4 | 6.03e-4 | 1.85e-4 | 1.09e-3 |
| 6.25e-3 | 3.77e-5 | 1.58e-4 | 4.16e-5 | 2.88e-4 |

TABLE 4.3

Relative errors using different time-steps for the predictor-corrector methods AB2*-AB3*, FE*-AB3*. The results in the first two columns refer to the PECE approach, while in the last two columns to the PEC approach.

| h | AB2*-AM3* | FE*-AM3* | AB2*-AM3* _{PEC} | FE*-AM3* _{PEC} |
|---------|-----------|----------|--------------------------|-------------------------|
| 2e-1 | 6.44e-2 | 4.07e-2 | NaN | 3.94e-2 |
| 1e-1 | 7.84e-3 | 2.02e-2 | 1.19e-2 | 2.91e-2 |
| 5e-2 | 2.67e-3 | 7.03e-3 | 3.75e-3 | 1.26e-2 |
| 2.5e-2 | 6.76e-4 | 2.07e-3 | 8.73e-4 | 4.02e-3 |
| 1.25e-2 | 1.62e-4 | 5.60e-4 | 1.91e-4 | 1.13e-3 |
| 6.25e-3 | 4.13e-5 | 1.47e-4 | 4.51e-5 | 2.98e-4 |

In Tables 4.2 and 4.3 we show relative errors for different predictor-corrector schemes. We note that the best performances are obtained using a second order predictor scheme with a PECE approach; for definition of PECE and PEC approach, see [16] or [24]. As expected, the differences between PECE approach and PEC are more evident when large time-steps are used.

5. Time adaptive strategy. Using an error estimate based on the PC scheme, we devise a time-adaptive strategy.

5.1. A posteriori error estimation. Our estimate for the error $\|y(t^{n+1}) - \hat{y}^{n+1}\|$ is based on the computed solutions y^{n+1} and \hat{y}^{n+1} ; for multistep methods this estimate is called Milne’s estimate; see [16]. We start considering a predictor-corrector couple of second order schemes, with parameters θ_p and θ_c , respectively. From (3.2) we have, for $i = 1, \dots, m$,

$$\begin{aligned}
 (5.1) \quad & y_i(t^{n+1}) - \hat{y}_i^{n+1} \\
 &= \left(\frac{1}{6} - \frac{\theta_p}{2}\right) (a_i''(t^n)y_i(t^n) - b_i''(t^n))h^3 + \frac{1}{12}(a_i'(t^n)b_i^n - a_i^n b_i'(t^n))h^3 + o(h^3), \\
 & y_i(t^{n+1}) - y_i^{n+1} \\
 &= \left(\frac{1}{6} - \frac{\theta_c}{2}\right) (a_i''(t^n)y_i(t^n) - b_i''(t^n))h^3 + \frac{1}{12}(a_i'(t^n)b_i^n - a_i^n b_i'(t^n))h^3 + o(h^3).
 \end{aligned}$$

Subtracting equation (5.1)₁ from (5.1)₂ we have

$$(5.2) \quad (a_i''(t^n)y_i(t^n) - b_i''(t^n))h^3 = \frac{2}{\theta_c - \theta_p} (y_i^{n+1} - \hat{y}_i^{n+1}) + o(h^3).$$

TABLE 5.1

Relative error using different time-steps for the predictor-corrector methods AB2-AB3*, FE*-AB3* corrected by local extrapolation. The results in the first two columns refer to the PECE approach, while in the last two columns to the PEC approach.*

| h | AB2*-CN _e * | AB2*-AM3 _e * | AB2*-CN _{e-PEC} * | AB2*-AM3 _{e-PEC} * |
|---------|------------------------|-------------------------|----------------------------|-----------------------------|
| 2e-1 | NaN | NaN | NaN | NaN |
| 1e-1 | 8.16e-3 | 8.06e-3 | 4.46e-3 | 4.59e-3 |
| 5e-2 | 3.84e-4 | 3.91e-4 | 1.91e-3 | 1.92e-3 |
| 2.5e-2 | 4.88e-5 | 4.91e-5 | 3.48e-4 | 3.49e-4 |
| 1.25e-2 | 7.03e-6 | 7.03e-6 | 4.97e-5 | 4.97e-5 |
| 6.25e-3 | 4.35e-6 | 4.35e-6 | 9.48e-6 | 9.48e-5 |

Substituting the latter equation into (5.1)₂, we have
 (5.3)

$$y_i(t^{n+1}) - y_i^{n+1} = \frac{\theta_c - \frac{1}{3}}{\theta_p - \theta_c} (y_i^{n+1} - \hat{y}_i^{n+1}) + \frac{1}{12} (a_i'(t^n) b_i^n - a_i^n b_i'(t^n)) h^3 + o(h^3).$$

In view of an *a posteriori* error estimator, the first derivatives of **a** and **b** can be approximated by forward differences,

$$a_i'(t^n) b_i^n - a_i^n b_i'(t^n) = \frac{1}{h} (a_i^{n+1} b_i^n - a_i^n b_i^{n+1}) + O(h).$$

Therefore, we obtain the error estimate
 (5.4)

$$y_i(t^{n+1}) - y_i^{n+1} = \boxed{\frac{\theta_c - \frac{1}{3}}{\theta_p - \theta_c} (y_i^{n+1} - \hat{y}_i^{n+1}) + \frac{1}{12} (a_i^{n+1} b_i^n - a_i^n b_i^{n+1}) h^2} + o(h^3).$$

For first order predictor-corrector pairs with $\omega_p \neq \omega_c$ (both $\neq 1/2$), we get the following error estimate,

$$(5.5) \quad \mathbf{y}(t^{n+1}) - \mathbf{y}^{n+1} = \boxed{\frac{\omega_c - \frac{1}{2}}{\omega_p - \omega_c} (\mathbf{y}^{n+1} - \hat{\mathbf{y}}^{n+1})} + o(h^2).$$

In principle, these estimates can be used to improve the solution to get a third order method (*local extrapolation*). As a matter of fact, once the error estimate \mathbf{E}^{n+1} is computed with the boxed terms above, we compute $\tilde{\mathbf{y}}^{n+1} = \mathbf{y}^{n+1} + \mathbf{E}^{n+1}$, raising by one the order of the method. In Table 5.1 we show relative errors of predictor-corrector schemes corrected with this *a posteriori* error estimation. We observe very slight differences between the schemes, the PECE approach performing better than the PEC approach. These schemes are more accurate than the second order ones (compare Table 5.1 with Tables 4.2 and 4.3), even if stability is affected by the extrapolation. Moreover, using this local extrapolation, we loose the favorable positivity properties of the non-corrected schemes.

5.2. Time adaptive schemes. Given a vector of tolerances $\boldsymbol{\tau}$ (possibly a different tolerance for each variable), we look for the largest time-step such that $E_i^n \leq \tau_i, i = 1, \dots, m$. Using a first order method $E_i^n \simeq K_i h^2$, where \mathbf{K} is a constant vector, if \mathbf{E}^n is the error obtained with a time-step h , then using a time-step $\tilde{h} = \min_i h \sqrt{\frac{\tau_i}{E_i^n}}$, we can obtain an error $\tilde{\mathbf{E}}$ such that $\tilde{E}_i^n \simeq \tau_i$ for some i . Similarly, using a second order method, the optimal time-step

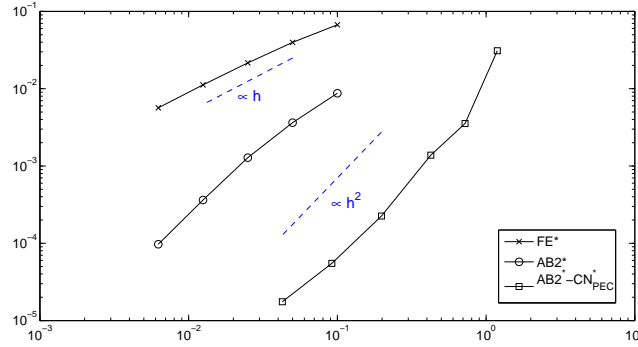


FIG. 5.1. Relative error curves as a function of the average step h , using the FE^* scheme, the $AB2^*$ scheme, and the time adaptive algorithm with the $AB2^*$ - CN^* scheme with PEC approach.

is given by $\tilde{h} = \min_i h \sqrt[3]{\frac{\tau_i}{E_i^n}}$; see [16]. In our simulations we weighted the tolerances based on the infinity norm of the components of the solution; hence, for the Luo-Rudy model from Figure 1.1, we get $\tau = \tau [84, 1, 1, 1, 1, 1, 1, 7e - 3]^T$. The time adapting algorithm reads, therefore

While $t^n < T$

1. Compute $\hat{\mathbf{y}}^{n+1}$ and \mathbf{y}^{n+1} with time-step h .
2. Compute the error \mathbf{E}^{n+1} .
3. If $E_i^{n+1} < \tau_i$ then $t^{n+1} = t^n + h$, $n + 1$.
4. Compute \tilde{h} , set $h = 0.95 \tilde{h}$ (0.95 is a precautionary parameter).

We define the recomputed percentage r as the percentage of the number of times the conditional expression 3 is false over the total number of steps n . Since the time-step is no longer constant, we need to recompute the coefficients of our scheme. In particular, if $\nu = \frac{h}{h_{old}}$ is the ratio between the time-step at the current iteration and the time-step at the previous iteration, we take $\tilde{c}_{-1} = c_{-1}$, $c_0 = c_0 + c_1(1 - \nu)$ and $\tilde{c}_1 = \nu c_1$ as the coefficient of the variable-step scheme. Writing the Taylor expansions for $a^{n+\frac{1}{2}}$ and $b^{n+\frac{1}{2}}$ and taking into account that $t^{n+1} - t^n = h^{n+1} = h$ and $t^n - t^{n-1} = h^n = \frac{h}{\nu}$, we obtain

$$(5.6) \quad \begin{aligned} \mathbf{a}^{n+\frac{1}{2}} &= \mathbf{a}^n + \tilde{\omega} \mathbf{a}'(t_n)h + \tilde{\theta} \mathbf{a}''(t_n) \frac{h^2}{2} + o(h^2), \\ \mathbf{b}^{n+\frac{1}{2}} &= \mathbf{b}^n + \tilde{\omega} \mathbf{b}'(t_n)h + \tilde{\theta} \mathbf{b}''(t_n) \frac{h^2}{2} + o(h^2), \end{aligned}$$

with $\tilde{\omega} = \tilde{c}_{-1} - \frac{\tilde{c}_1}{\nu} = \omega$ and $\tilde{\theta} = \tilde{c}_{-1} + \frac{\tilde{c}_1}{\nu^2}$. The local truncation error expressions (3.1), (3.2), and error estimates (5.4) and (5.5) still hold when θ is replaced with $\tilde{\theta}$.

REMARK 5.1. From now on we will consider only a second order time-adaptive PC method. First order methods are used only in the first step, whose errors are estimated by (5.5). In particular, we use FE^* as predictor and BE (Backward Euler) as corrector.

We solve the Luo-Rudy system with our time-adaptive algorithm. More precisely, we select the predictor to be $AB2^*$ and use different correctors, namely $AM3^*$, CN^* , and $M(0.6)^*$. Results are shown in Table 5.2. $M(0.6)^*$ is more stable than CN^* even if slightly less accurate.

In Figure 5.1, we compare the error curves as a function of the average step h , using the Rush-Larsen scheme, the $AB2^*$ scheme, and the time adaptive algorithm with the $AB2^*$ - CN^* scheme with PEC approach.

TABLE 5.2

Average time-step h , recomputed percentage r , and relative error of the solution computed using different predictor-corrector methods with time adaptive strategy for different values of tolerance τ .

| τ | AB2*-AM3* | | | AB2*-CN* | | | AB2*-M(0.6)* | | |
|--------|-----------|-----|---------|----------|-----|---------|--------------|-----|---------|
| | h | r | err | h | r | err | h | r | err |
| 2.5e-2 | 1.25 | 3% | 4.18e-2 | 1.23 | 4% | 3.65e-2 | 1.24 | 3% | 3.91e-2 |
| 5e-3 | 7.29e-1 | 3% | 3.21e-3 | 7.23e-1 | 3% | 2.94e-3 | 7.25e-1 | 3% | 3.44e-2 |
| 1e-3 | 4.27e-1 | 2% | 2.18e-3 | 4.25e-1 | 3% | 9.09e-4 | 4.24e-1 | 2% | 4.90e-3 |
| 1e-4 | 1.99e-1 | 1% | 5.58e-4 | 1.98e-1 | 1% | 2.31e-4 | 1.97e-1 | 1% | 5.58e-4 |
| 1e-5 | 9.25e-1 | 8‰ | 1.14e-4 | 9.19e-2 | 6‰ | 7.31e-5 | 9.17e-2 | 7‰ | 1.42e-4 |
| 1e-6 | 4.30e-1 | 6‰ | 2.43e-5 | 4.27e-2 | 3‰ | 1.96e-5 | 4.26e-2 | 2‰ | 3.64e-5 |

TABLE 5.3

Average time-step h , recomputed percentage r , and relative error of the solution computed using the predictor-corrector method AB2-CN* with time adaptive strategy for different values tolerance τ . From left to right, the solution is computed, respectively, with a PEC approach, with a PECE approach and local extrapolation, with PEC approach and local extrapolation.*

| 4τ | AB2*-CN* _{PEC} | | | AB2*-CN* _e | | | AB2*-CN* _{e-PEC} | | |
|---------|-------------------------|-----|---------|-----------------------|-----|---------|---------------------------|-----|---------|
| | h | r | err | h | r | err | h | r | err |
| 2.5e-2 | 1.19 | 10% | 3.10e-2 | 1.18 | 8% | 2.51e-2 | 1.20 | 9% | 2.22e-2 |
| 5e-3 | 7.22e-1 | 4% | 3.54e-3 | 7.22e-1 | 4% | 4.73e-3 | 7.22e-1 | 3% | 7.28e-3 |
| 1e-3 | 4.25e-1 | 2% | 1.38e-3 | 4.25e-1 | 2% | 9.30e-4 | 4.25e-1 | 2% | 2.75e-3 |
| 1e-4 | 1.98e-1 | 1% | 2.25e-4 | 1.98e-1 | 1% | 1.19e-4 | 1.98e-2 | 1e% | 4.13e-4 |
| 1e-5 | 9.19e-2 | 7‰ | 5.50e-5 | 9.19e-2 | 7‰ | 1.48e-5 | 9.19e-2 | 7‰ | 4.79e-5 |
| 1e-6 | 4.27e-2 | 3‰ | 1.75e-5 | 4.27e-2 | 3‰ | 1.66e-6 | 4.27e-2 | 3‰ | 5.13e-6 |

6. Monodomain and bidomain systems. The bidomain model is one of the most popular and accurate model to describe the propagation of action potential in the myocardium. A mathematical derivation of the bidomain model is discussed in [9]. Well-posedness analysis results on bidomain system coupled with different ionic models are presented in [27, 28], while several simulations of the action potential propagation using monodomain and bidomain systems can be found in [7, 8]. A possible formulation of the problem reads

$$(6.1) \quad \left\{ \begin{array}{ll}
 \frac{\partial u}{\partial t} - \frac{1}{\chi C_m} \nabla \cdot \left(\frac{\lambda \mathbf{D}_i}{1 + \lambda} \nabla u \right) - \frac{1}{\chi C_m} \nabla \cdot \left(\frac{\lambda \mathbf{D}_i - \mathbf{D}_e}{1 + \lambda} \nabla u^e \right) = I & \text{in } \Omega \times (0, T], \\
 -\nabla \cdot [\mathbf{D}_i \nabla u + (\mathbf{D}_i + \mathbf{D}_e) \nabla u^e] = \chi \tilde{I}_{app} & \text{in } \Omega \times (0, T], \\
 \mathbf{n}^T \mathbf{D}_i (\nabla u + \nabla u^e) = 0 & \text{on } \partial\Omega \times (0, T], \\
 \mathbf{n}^T \mathbf{D}_e \nabla u^e = 0 & \text{on } \partial\Omega \times (0, T], \\
 \int_{\Omega} u^e dx = 0 & \text{in } (0, T], \\
 u(\mathbf{x}, 0) = u_0, \quad u^e(\mathbf{x}, 0) = 0 & \text{in } \Omega,
 \end{array} \right.$$

with the ionic current equations

$$(6.2) \quad \begin{cases} \frac{\partial \mathbf{X}}{\partial t} = \mathbf{g}(u, \mathbf{X}, \mathbf{w}) & \text{in } \Omega \times (0, T], \\ \frac{\partial w_i}{\partial t} = a_i(u)w_i + b_i(u) & \text{in } \Omega \times (0, T], \\ \mathbf{X}(\mathbf{x}, 0) = \mathbf{X}_0, \mathbf{w}(\mathbf{x}, 0) = \mathbf{w}_0 & \text{in } \Omega. \end{cases}$$

Here Ω is the spatial domain, u^e is the extracellular potential, \mathbf{D}^i and \mathbf{D}^e are the intracellular and extracellular conductivity tensors, and χ the membrane area per unit tissue. The source terms \tilde{I}_{app} and I are defined, respectively, as $\tilde{I}_{app} = I_{app}^i + I_{app}^e$ and $I = \frac{1}{C_m} \left(\frac{\lambda I_{app}^i - I_{app}^e}{\lambda + 1} - I_{ion} \right)$, where I_{app}^i and I_{app}^e are the applied intracellular and the extracellular current stimuli. The current stimuli must satisfy the compatibility condition $\int_{\Omega} (I_{app}^i + I_{app}^e) d\mathbf{x} = 0$. In the sequel we take $I_{app}^i = -I_{app}^e = I^{app}$. The coefficient λ is chosen in such a way that $\lambda \mathbf{D}_i \simeq \mathbf{D}_e$ in order to weaken the coupling between the first and the second equation. Under the (in general not realistic) assumption that the conductivity tensors \mathbf{D}_i and \mathbf{D}_e are proportional, the bidomain system can be reduced to the monodomain system, and computation of u and u^e is decoupled. The monodomain system reads

$$(6.3) \quad \begin{cases} \frac{\partial u}{\partial t} - \nabla \cdot (\mathbf{D}^M \nabla u) = I & \text{in } \Omega \times (0, T], \\ \mathbf{n}^T \mathbf{D}^M \nabla u = 0 & \text{on } \partial\Omega \times (0, T], \end{cases}$$

together with (6.2) and the initial condition $u(\mathbf{x}, 0) = u_0(\mathbf{x})$. Here $\mathbf{D}^M = \frac{1}{\chi C_m} \frac{\lambda \mathbf{D}_i}{1 + \lambda}$ is the conductivity tensor and I is defined as $I = \frac{1}{C_m} (I_{app} - I_{ion})$.

6.1. Monodomain model discretization. In the time discretization of (6.3) we treat implicitly the diffusion term in order to avoid small time-steps. Usually the monodomain system is discretized as

$$(6.4) \quad \begin{cases} \frac{1}{h} u^{n+1} - \nabla \cdot (\mathbf{D}^M \nabla u^{n+1}) = \frac{1}{h} u^n + I^n, \\ \frac{1}{h} w_i^{n+1} = \frac{1}{h} w_i^n + \Phi(a_i^n h) (a_i^n w_i^n + b_i^n), \quad i = 1, \dots, m, \\ \frac{1}{h} \mathbf{X}^{n+1} = \frac{1}{h} \mathbf{X}^n + \mathbf{g}^n, \end{cases}$$

for $n = 0, \dots, N$. The PDE is solved by a SBDF scheme, an IMEX [13, 5] method which combines Backward Euler with FE schemes. The gate variables are solved by the Rush-Larsen method and the concentration variables by FE. We call this method SBDF-FE*. Another common discretization of the monodomain model is to replace, in the first equation of system (6.4), I^n by $I(u^n, \mathbf{w}^{n+1}, \mathbf{X}^{n+1})$. Since this is similar to a Gauss-Seidel substitution approach, we call this method SBDF-FE*-GS.

A second order scheme can be achieved using the AB2* scheme for the gate equations, AB2 for the concentration equations, and a second order IMEX scheme for the PDEs. We choose the CNAB scheme, combining the CN scheme for the diffusion term and AB2 for the forcing term (according to [5] the CNAB scheme is effective for solving the monodomain

equation). In this case the discrete system reads

$$(6.5) \quad \begin{cases} \frac{1}{h}u^{n+1} - \frac{1}{2}\nabla \cdot (\mathbf{D}^M \nabla u^{n+1}) = \frac{1}{h}u^n + \frac{1}{2}\nabla \cdot (\mathbf{D}^M \nabla u^n) + \frac{3}{2}I^n - \frac{1}{2}I^{n-1}, \\ \frac{1}{h}w_i^{n+1} = \frac{1}{h}w_i^n + \Phi(a_i^{n+\frac{1}{2}}h) \left(a_i^{n+\frac{1}{2}}w_i^n + b_i^{n+\frac{1}{2}} \right), \quad i = 1, \dots, m, \\ \frac{1}{h}\mathbf{X}^{n+1} = \frac{1}{h}\mathbf{X}^n + \frac{3}{2}\mathbf{g}^n - \frac{1}{2}\mathbf{g}^{n-1}, \end{cases}$$

for $n = 1, \dots, N$, where we set $I^{-1} = I^0$, $\mathbf{g}^{-1} = \mathbf{g}^0$, and $\mathbf{a}^{n+\frac{1}{2}}$, $\mathbf{b}^{n+\frac{1}{2}}$ are chosen as in (2.6) with $c_{-1} = 0$, $c_0 = \frac{3}{2}$, and $c_1 = -\frac{1}{2}$.

This scheme becomes unstable for time-steps larger than 1 *ms* and oscillations persist for time-steps larger than 0.5 *ms*. In order to overcome these problems and reduce at the same time computational efforts, we apply our time adaptive scheme. We still treat the diffusion term implicitly also in the corrector scheme. This procedure does not affect the error estimate, since (3.1), (3.2), (5.4), (5.5) still hold. The entire time-discretized monodomain problem reads

$$(6.6) \quad \begin{cases} P : \begin{cases} \frac{1}{h}\hat{u}^{n+1} = \frac{1}{h}u^n + \bar{c}_0 \nabla \cdot (\mathbf{D}^M \nabla u^n) + \bar{c}_1 \nabla \cdot (\mathbf{D}^M \nabla u^{n-1}) + \bar{c}_0 I^n + \bar{c}_1 I^{n-1}, \\ \frac{1}{h}\hat{w}_i^{n+1} = \frac{1}{h}w_i^n + \Phi(\bar{a}_i^{n+\frac{1}{2}}h) \left(\bar{a}_i^{n+\frac{1}{2}}w_i^n + \bar{b}_i^{n+\frac{1}{2}} \right), \quad i = 1, \dots, m, \\ \frac{1}{h}\hat{\mathbf{X}}^{n+1} = \frac{1}{h}\mathbf{X}^n + \bar{c}_0 \mathbf{g}^n + \bar{c}_1 \mathbf{g}^{n-1}, \end{cases} \\ C : \begin{cases} \frac{1}{h}u^{n+1} - c_{-1} \nabla \cdot (\mathbf{D}^M \nabla u^{n+1}) = \\ \quad \frac{1}{h}u^n + c_0 \nabla \cdot (\mathbf{D}^M \nabla u^n) + c_1 \nabla \cdot (\mathbf{D}^M \nabla u^{n-1}) + c_{-1}\hat{I}^{n+1} + c_0 I^n + c_1 I^{n-1}, \\ \frac{1}{h}w_i^{n+1} = \frac{1}{h}w_i^n + \Phi(\hat{a}_i^{n+\frac{1}{2}}h) \left(\hat{a}_i^{n+\frac{1}{2}}w_i^n + \hat{b}_i^{n+\frac{1}{2}} \right), \quad i = 1, \dots, m, \\ \frac{1}{h}\mathbf{X}^{n+1} = \frac{1}{h}\mathbf{X}^n + c_{-1}\hat{\mathbf{g}}^{n+1} + c_0 \mathbf{g}^n + c_1 \mathbf{g}^{n-1}, \end{cases} \end{cases}$$

for $n = 1, \dots, N$, where \hat{I}^{n+1} and $\hat{\mathbf{g}}^{n+1}$ are computed using the predictor solutions \hat{u}^{n+1} , $\hat{\mathbf{w}}^{n+1}$, $\hat{\mathbf{X}}^{n+1}$, and $\bar{\mathbf{a}}^{n+\frac{1}{2}}$, $\bar{\mathbf{b}}^{n+\frac{1}{2}}$, $\bar{\mathbf{a}}^{n+\frac{1}{2}}$, and $\bar{\mathbf{a}}^{n+\frac{1}{2}}$ are defined as in (4.5). We solve the system (4.4) for the 1D Luo-Rudy model. Space discretization is carried out with a Galerkin linear finite element method. This choice is motivated in view of extending these computations to the 3D case. We consider $\Omega = (0, l)$ and introduce the grid points $\{x_k\}_0^{N_e}$ given by $x_k = k \delta x$, where $\delta x = \frac{l}{N_e}$ is the grid spacing. We approximate y_i^n with $(y_h^n)_i = \sum_{k=0}^{N_e} \tilde{y}_{i,k}^n \varphi_k$, where $\{\varphi_k\}_0^{N_e}$ is the Lagrangian base for the space of piecewise linear continuous functions on Ω . We define the 1D $L^2(\Omega)$ norm with a trapezoidal rule, namely,

$$\|(y_h^n)_i\| = \sqrt{\frac{1}{2} \sum_{k=0}^{M-1} \left[\left(\tilde{y}_{i,k}^n \right)^2 + \left(\tilde{y}_{i,k+1}^n \right)^2 \right] \delta x}.$$

We refer then to the space-time norm $\|(y_h^n)_i\|_{st}$ corresponding to the space $L^2(0, T; L^2(\Omega))$.

The relative error is given by $\max_i \frac{\|(y_h^n)_i - y_i(x_k, t^n)\|_{st}}{\|y_i(x_k, t^n)\|_{st}}$. Unless stated otherwise, in the following simulations, we take $T = 500$, $l = 5cm$, $N_e = 500$ and

$$(6.7) \quad I_{app}(t, x) = \begin{cases} I_{max} \left(\frac{1}{2} - \frac{1}{2} \cos \left(2\pi \frac{t}{t_p} \right) \right), & t < t_p, x < x_p, \\ 0, & \text{otherwise,} \end{cases}$$

where $I_{max} = 60\mu A$, $t_p = 1ms$ and $x_p = 1.5mm$. As reference solution we consider the one obtained using the predictor-corrector scheme AB2*-CN*, adapted in time, with $\tau = 1e-9$ and $N_e = 500$. We are interested in time discretization errors, hence, the reference

TABLE 6.1

Relative errors using different time-steps for the methods SBDF-FE*, SBDF-FE*-GS, and CNAB-AB2*. The results in the first two columns refer to the PECE approach, while in the last two columns to the PEC approach.

| h | SBDF-FE* | SBDF-FE*-GS | CNAB-AB2* |
|---------|----------|-------------|-----------|
| 2e-1 | 4.47e-1 | 5.14e-2 | NaN |
| 1e-1 | 3.09e-1 | 6.85e-2 | 4.67e-2 |
| 5e-2 | 2.12e-1 | 5.71e-2 | 4.24e-2 |
| 2.5e-2 | 1.48e-1 | 3.71e-2 | 1.86e-2 |
| 1.25e-2 | 1.02e-1 | 2.17e-2 | 5.52e-3 |
| 6.25e-3 | 6.59e-2 | 1.18e-2 | 1.46e-3 |

TABLE 6.2

Average time-step h , recomputed percentage r , and relative error of the solution for the monodomain model, computed using different predictor-corrector methods with time adaptive strategy.

| τ | AB2*-CN* | | | AB2*-CN* _{PEC} | | | AB2*-M(0.6)* _{PEC} | | |
|--------|----------|-----|---------|-------------------------|-----|---------|-----------------------------|-----|---------|
| | h | r | err | h | r | err | h | r | err |
| 1e-1 | 5.92e-1 | 1% | 2.57e-1 | 4.78e-1 | 7% | 1.71e-1 | 4.87e-1 | 28% | 9.53e-2 |
| 2.5e-2 | 3.63e-1 | 6% | 3.96e-2 | 3.43e-1 | 9% | 4.04e-2 | 3.42e-1 | 15% | 3.19e-2 |
| 5e-3 | 2.14e-1 | 6% | 2.90e-2 | 2.11e-1 | 8% | 2.70e-2 | 2.14e-1 | 7% | 2.13e-2 |
| 1e-3 | 1.26e-1 | 6% | 1.34e-2 | 1.26e-1 | 5% | 1.30e-2 | 1.24e-1 | 13% | 1.10e-2 |
| 1e-4 | 5.70e-2 | 11% | 3.14e-3 | 5.77e-2 | 7% | 3.06e-3 | 5.53e-2 | 17% | 2.67e-3 |
| 1e-5 | 2.62e-2 | 11% | 6.21e-4 | 2.62e-2 | 10% | 6.20e-4 | 2.55e-2 | 17% | 6.13e-4 |

solution is computed on the same grid used for the other numerical solutions. In Table 6.1 we report results obtained for different time-steps, using the SBDF-FE*, SBDF-FE*-GS, and CNAB-AB2* schemes. In Table 6.2 we report results obtained with the AB2*-CN* scheme and the predictor-corrector scheme AB2*-M(0.6)*. In Figure 6.1 we report relative error curves as a function of the average time-step h , using the SBDF-FE* scheme, the CNAB-AB2* scheme, and the time adaptive algorithm with the AB2*-CN* scheme. Second order methods with $\theta < \frac{1}{2}$ used as correctors and methods corrected with local extrapolation present instabilities.

Our numerical methods are robust with respect to the spatial resolution as shown in Table 6.3, where we compare the average time-step h , the recomputed percentage r , and the relative error for different mesh sizes. The reference solutions are computed using the different grids and taking a tolerance defined as $\tau = 1e - 9$. The recomputed percentage increases on coarse grids, while h and the errors are fairly insensitive.

TABLE 6.3

Average time-step h , recomputed percentage r , and relative error of the solution for the monodomain model, computed on different grids, using AB2*-CN*_{PEC} scheme with time adaptive strategy.

| τ | AB2*-CN* _{PEC} , $\delta x = \frac{5}{125}$ | | | AB2*-CN* _{PEC} , $\delta x = \frac{5}{250}$ | | | AB2*-CN* _{PEC} , $\delta x = \frac{5}{500}$ | | |
|--------|--|-----|---------|--|-----|---------|--|-----|---------|
| | h | r | err | h | r | err | h | r | err |
| 1e-1 | 5.18e-1 | 30% | 1.57e-1 | 4.80e-1 | 18% | 2.11e-1 | 4.78e-1 | 7% | 1.71e-1 |
| 2.5e-2 | 3.58e-1 | 27% | 5.97e-2 | 3.55e-1 | 16% | 3.11e-2 | 3.43e-1 | 9% | 4.04e-2 |
| 5e-3 | 2.21e-1 | 22% | 5.32e-2 | 2.15e-1 | 9% | 3.56e-2 | 2.11e-1 | 8% | 2.70e-2 |
| 1e-3 | 1.31e-1 | 10% | 2.30e-2 | 1.27e-1 | 8% | 1.65e-2 | 1.26e-1 | 5% | 1.30e-2 |
| 1e-4 | 6.10e-2 | 8% | 3.69e-3 | 5.89e-2 | 3% | 3.56e-3 | 5.77e-2 | 7% | 3.06e-3 |
| 1e-5 | 2.82e-2 | 4% | 5.33e-4 | 2.71e-2 | 5% | 6.77e-4 | 2.62e-2 | 10% | 6.20e-4 |

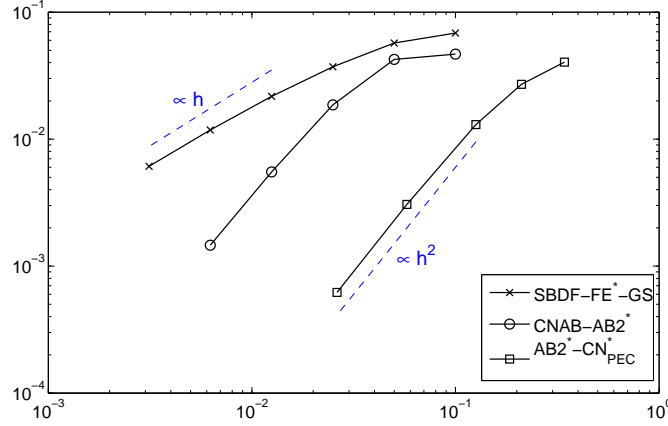


FIG. 6.1. Relative error curves as a function of the average step h , using the SBDP-FE* scheme, the CNAB-AB2* scheme, and the time adaptive algorithm with the AB2*-CN* scheme with PEC approach.

REMARK 6.1. *The 3D bidomain problem.* A complete analysis of the results of our solver coupled with the (2D-3D) bidomain complete model is beyond the scope of the present work. However, we want to address briefly a possible strategy for an efficient coupling of the PDE solver and our method. Usually, the bidomain system is written in a symmetric form featuring the two variables u^i and u^e , where $u^i = u + u^e$ is the intracellular potential. However, if we resort to the non-symmetric form, in the predictor step we can avoid solving the second equation of the system. The time-discretized problem reads, for $n = 1, \dots, N$,

$$(6.8) \quad \begin{cases} P : \begin{cases} \frac{1}{h} \hat{u}^{n+1} = \frac{1}{h} u^n + \bar{c}_0 \nabla \cdot (\mathbf{D}^M \nabla u^n) + \bar{c}_1 \nabla \cdot (\mathbf{D}^M \nabla u^{n-1}) \\ \quad + \bar{c}_0 \nabla \cdot (\mathbf{D}^\Delta \nabla (u^e)^n) + \bar{c}_1 \nabla \cdot (\mathbf{D}^\Delta \nabla (u^e)^{n-1}) + \bar{c}_0 I^n + \bar{c}_1 I^{n-1}, \\ \frac{1}{h} \hat{w}_i^{n+1} = \frac{1}{h} w_i^n + \Phi(\bar{a}_i^{n+\frac{1}{2}} h) \left(\bar{a}_i^{n+\frac{1}{2}} w_i^n + \bar{b}_i^{n+\frac{1}{2}} \right), \\ \frac{1}{h} \hat{\mathbf{X}}^{n+1} = \frac{1}{h} \mathbf{X}^n + \bar{c}_0 \mathbf{g}^n + \bar{c}_1 \mathbf{g}^{n-1}, \end{cases} \\ C : \begin{cases} \frac{1}{h} u^{n+1} - c_{-1} \nabla \cdot (\mathbf{D}^M \nabla u^{n+1}) - c_{-1} \nabla \cdot (\mathbf{D}^\Delta \nabla (u^e)^{n+1}) \\ \quad = \frac{1}{h} u^n + c_0 \nabla \cdot (\mathbf{D}^M \nabla u^n) + c_1 \nabla \cdot (\mathbf{D}^M \nabla u^{n-1}) + c_0 \nabla \cdot (\mathbf{D}^\Delta \nabla (u^e)^n) \\ \quad \quad + c_1 \nabla \cdot (\mathbf{D}^\Delta \nabla (u^e)^{n-1}) + c_{-1} \hat{I}^{n+1} + c_0 I^n + c_1 I^{n-1}, \\ -\nabla \cdot [\mathbf{D}_i \nabla u^{n+1} + (\mathbf{D}_i + \mathbf{D}_e) \nabla (u^e)^{n+1}] = 0, \\ \int_{\Omega} (u^e)^{n+1} d\mathbf{x} = 0, \\ \frac{1}{h} w_i^{n+1} = \frac{1}{h} w_i^n + \Phi(\hat{a}_i^{n+\frac{1}{2}} h) \left(\hat{a}_i^{n+\frac{1}{2}} w_i^n + \hat{b}_i^{n+\frac{1}{2}} \right), \\ \frac{1}{h} \mathbf{X}^{n+1} = \frac{1}{h} \mathbf{X}^n + c_{-1} \hat{\mathbf{g}}^{n+1} + c_0 \mathbf{g}^n + c_1 \mathbf{g}^{n-1}, \end{cases} \end{cases}$$

where $\mathbf{D}^\Delta = \frac{1}{\chi C_m} \frac{\lambda \mathbf{D}_i - \mathbf{D}_e}{1 + \lambda}$. The terms \hat{I}^{n+1} , $\hat{\mathbf{g}}^{n+1}$, \bar{a}^n , \bar{b}^n , \hat{a}^n , \hat{b}^n are defined as in the system (6.6).

Most of the computational effort is required by the solution of the PDE system in the corrector step. An efficient way to solve this system is presented in [10]. A detailed analysis of 3D bidomain results with our method is presented elsewhere; see [21].

7. Conclusions. We presented a generalization to the popular Rush-Larsen method used for solving nonlinear ordinary differential systems for the ionic dynamics in electro-physiology,

in particular for the cardiac potential propagation. We extended the method to a class of second order schemes. These schemes fall into the set of exponential integrators, even if peculiar linearization performed in their formulation makes them different from other schemes previously proposed.

These methods also can be regarded as a generalization of classical multistep methods whenever the problem at hand is naturally split into a linear and a nonlinear part. We have carried out the analysis of the schemes, including the Rush-Larsen scheme which to the best of our knowledge has not been analyzed before. One of the relevant properties of these methods is that they can preserve bounds for the solution. Analysis shows that the approach pursued here improves the absolute stability properties of the corresponding multistep scheme, as numerical results confirm. The major limitation of our approach at this time is the accuracy, which is limited to the second order as a consequence of the linearization procedure. Nevertheless, the methods are accurate enough to be used in realistic electro-cardiology simulations.

We presented an extensive discussion of the predictor-corrector formulation of our method for problems in electro-physiology and on the time-adaptive implementation, which is of paramount relevance in cardiac applications. Preliminary results carried out on a simplified 1D model for cardiac potential confirm the effectiveness of our approach in view of more realistic simulations over 3D domains.

Appendix A. We describe the Luo-Rudy model phase I [17]. The variables \mathbf{w} , \mathbf{X} , and functions I , \mathbf{a} , \mathbf{b} , and \mathbf{g} of the system (1.1) are specified as follows. We made slight modifications of the original model in functions α_h , β_h , α_j , β_j , and X_i in order to make them continuous. The modifications are only of the inequalities on u .

$$\begin{aligned}
 \mathbf{w} &= [h \ j \ m \ d \ f \ X]^T, \\
 \mathbf{a} &= -[(\alpha_h + \beta_h), (\alpha_j + \beta_j), (\alpha_m + \beta_m), (\alpha_d + \beta_d), (\alpha_f + \beta_f), (\alpha_X + \beta_X)]^T, \\
 \mathbf{b} &= [\alpha_h \ \alpha_j \ \alpha_m \ \alpha_d \ \alpha_f \ \alpha_X]^T, \\
 \mathbf{X} &= [Ca], \quad \mathbf{g} = -10^{-4}I_{si} + 0.07(10^{-4} - Ca), \\
 I_{ion} &= I_{K1} + I_{Kp} + I_b + I_K + I_{Na} + I_{si}, \\
 u_0 &= -84mV, \quad \mathbf{X}_0 = 2e - 4mM, \quad \mathbf{w}_0 = [1 \ 1 \ 0 \ 0 \ 1 \ 0]^T,
 \end{aligned}$$

where the gating functions are defined as follows:

$$\begin{aligned}
 I_{Na} &= 23 \ m^3 \ h \ j \ (u - E_{Na}), & E_{Na} &= 54.4mV, \\
 \alpha_h &= 0.135e^{-\frac{80+u}{6.8}}, \\
 \beta_h &= \begin{cases} 0.13 \left(1 + e^{-\frac{u+10.66}{11.1}}\right), & u \geq -38.7381, \\ 3.56e^{0.079u} + 3.1 \cdot 10^5 e^{0.35u}, & u < -38.7381, \end{cases} \\
 \alpha_j &= \begin{cases} \frac{(u + 37.78) (-1.2714 \cdot 10^5 e^{0.2444u} - 3.474 \cdot 10^{-5} e^{-0.04391u})}{1 + e^{0.311(u+79.23)}}, & u < -37.78, \\ 0, & u \geq -37.78, \end{cases} \\
 \beta_j &= \begin{cases} \frac{0.3e^{2.535 \cdot 10^{-7}u}}{1 + e^{-0.1(u+32)}}, & u \geq -39.826, \\ \frac{0.1212e^{-0.01052u}}{1 + e^{-0.1378(u+40.14)}}, & u < -39.826, \end{cases}
 \end{aligned}$$

$$\begin{aligned}
 \alpha_m &= 0.32 \frac{u + 47.13}{1 - e^{-0.1(u+47.13)}}, & \beta_m &= 0.08e^{-\frac{u}{11}}, \\
 \alpha_d &= 0.095 \frac{e^{-0.01(u-5)}}{1 + e^{-0.072(u-5)}}, & \beta_d &= 0.07 \frac{e^{-0.017(u+44)}}{1 + e^{0.05(u+44)}}, \\
 \alpha_f &= 0.012 \frac{e^{-0.008(u+28)}}{1 + e^{0.15(u+28)}}, & \beta_f &= 0.0065 \frac{e^{-0.02(u+30)}}{1 + e^{-0.2(u+30)}}, \\
 \alpha_X &= 0.0005 \frac{e^{0.083(u+50)}}{1 + e^{0.057(u+50)}}, & \beta_X &= 0.0013 \frac{e^{-0.06(u+20)}}{1 + e^{-0.04(u+20)}}.
 \end{aligned}$$

Ionic currents are defined as follows:

$$\begin{aligned}
 I_{si} &= 0.09 d f(u - E_{si}), \\
 E_{si} &= 7.7 - 13.0287 \ln(Ca), \\
 I_K &= \overline{G}_K X X_i (u - E_K), \quad E_K = -77.01 mV, \quad \overline{G}_K = 0.282 \sqrt{\frac{K_o}{5.4}}, \quad K_o = 5.4 mM, \\
 X_i &= \begin{cases} 2.837 \frac{e^{0.04(u+77)} - 1}{(u + 77)e^{0.04(u+35)}}, & u > -100.05, \\ 1, & u \leq -100.05, \end{cases} \\
 I_{K1} &= \overline{G}_{K1} \frac{\alpha_{K1}}{\alpha_{K1} + \beta_{K1}} (u - E_{K1}), \quad E_{K1} = -87.26 mV, \quad \overline{G}_{K1} = 0.282 \sqrt{\frac{K_o}{5.4}}, \\
 \alpha_{K1} &= 1.02 \frac{1}{1 + e^{0.2385(u - E_{K1} - 59.215)}}, \\
 \beta_{K1} &= \frac{0.49124 e^{0.08032(u - E_{K1} + 5.476)} + e^{0.06175(u - E_{K1} - 594.31)}}{1 + e^{-0.5143(u - E_{K1} + 4.753)}}, \\
 I_{Kp} &= 0.0183 K_p (u - E_{Kp}), \quad E_{Kp} = E_{K1}, \\
 K_p &= \frac{1}{1 + e^{\frac{7.488 - u}{5.98}}}, \\
 I_b &= 0.03921 (u + 59.87),
 \end{aligned}$$

Acknowledgments. The authors thank Marta D’Elia for her helpful comments in preparing this work.

REFERENCES

- [1] G. W. BEELER AND H. REUTER, *Reconstruction of the action potential of ventricular myocardial fibres*, J. Physiol., 268 (1977), p. 177–210.
- [2] G. BEYLKIN, J. M. KEISER, AND L. VOZOVoi, *A new class of time discretization schemes for the solution of nonlinear PDEs*, J. Comput. Phys., 147 (1998), pp. 362–387.
- [3] E. M. CHERRY, H. S. GREENSIDE, AND C. S. HENRIQUEZ, *A space-time adaptive method for simulating complex cardiac dynamics*, Phys. Rev. Lett., 84 (2000), pp. 1343–1346.
- [4] M. COURTEMANCHE, R. J. RAMIREZ, AND S. NATTEL, *Ionic mechanisms underlying human atrial action potential properties: insights from a mathematical model*, Am. J. Physiol. Heart Circ. Physiol., 275 (1998), pp. H301–H321.
- [5] M. ETHIER AND Y. BOURGAULT, *Semi-Implicit Time-Discretization schemes for the bidomain model*, SIAM J. Numer. Anal., 46 (2008), pp. 2443–2468.
- [6] P. C. FRANZONE, P. DEUFLHARD, B. ERDMANN, J. LANG, AND L. F. PAVARINO, *Adaptivity in space and time for reaction-diffusion systems in electrocardiology*, SIAM J. Sci. Comput., 28 (2006), pp. 942–962.
- [7] P. C. FRANZONE AND L. F. PAVARINO, *A parallel solver for reaction-diffusion systems in computational electrocardiology*, Math. Models Methods Appl. Sci., 14 (2004), pp. 883–911.
- [8] P. C. FRANZONE, L. F. PAVARINO, AND B. TACCARDI, *Simulating patterns of excitation, repolarization and action potential duration with cardiac bidomain and monodomain models*, Math. Biosci., 197 (2005), pp. 35–66.

- [9] P. C. FRANZONE AND G. SAVARÉ, *Degenerate evolution systems modeling the cardiac electric field at micro and macroscopic level*, in *Evolution Equations Semigroups and Functional Analysis*, A. Lorenzi and B. Ruff, eds., Birkhauser, Basel - Boston - Berlin, 2002, pp. 218–240.
- [10] L. GERARDO-GIORDA, L. MIRABELLA, F. NOBILE, M. PEREGO, AND A. VENEZIANI, *A model-based block-triangular preconditioner for the bidomain system in electrocardiology*, *J. Comput. Phys.*, 228 (2009), pp. 3625–3639.
- [11] A. L. HODGKIN AND A. F. HUXLEY, *A quantitative description of membrane current and its application to conduction and excitation in nerve*, *J. Physiol.*, 117 (1952), pp. 500–544.
- [12] W. HUNSDORFER, S. J. RUUTH, AND R. J. SPITERI, *Monotonicity-preserving linear multistep methods*, *SIAM J. Numer. Anal.*, 41 (2003), pp. 605–623.
- [13] W. HUNSDORFER AND J. VERWER, *Numerical Solution of Time-Dependent Advection-Diffusion-Reaction Equations*, Vol. 33, Springer Series in Computational Mathematics, Springer, Berlin - Heidelberg - New York, 2003.
- [14] M. S. JAFRI, J. J. RICE, AND R. L. WINSLOW, *Cardiac ca^{2+} dynamics: the roles of ryanodine receptor adaptation and sarcoplasmic reticulum load*, *Biophys. J.*, 74 (1998), pp. 1149–1168.
- [15] G. E. KARNIADAKIS, M. ISRAELI, AND S. A. ORSZAG, *High-order splitting methods for the incompressible Navier-Stokes equations*, *J. Comput. Phys.*, 97 (1991), pp. 414–443.
- [16] J. D. LAMBERT, *Numerical Methods For Ordinary Differential Systems*, John Wiley & Sons, New York, 1991.
- [17] L. LUO AND Y. RUDY, *A model of the ventricular cardiac action potential: depolarization, repolarization and their interaction*, *Circ. Res.*, 68 (1991), pp. 1501–1526.
- [18] B. A. MINCHEV AND W. M. WRIGHT, *A review of exponential integrators for first order semilinear problems*, Tech. Report 2/05, Department of Mathematics, Norwegian University of Science and Technology, (2005).
- [19] S. NØRSETT, *An a -stable modification of the Adams-Bashforth methods*, in *Conference on the Numerical Solution of Differential Equations*, J. Ll. Morris, ed., Dundee, Scotland, June 23-27, 1969, Lecture Notes in Math., Vol. 109, Springer, Berlin - Heidelberg, 1969, pp. 214–219.
- [20] A. OSTERMANN AND M. THALHAMMER, *Positivity of exponential multistep methods*, in *Numerical Mathematics and Advanced Applications, ENUMATH 2005*, A. Bermudez, D. Gómez, P. Quintela, and P. Sagado, eds., Springer, Berlin, 2006, pp. 564–571.
- [21] M. PEREGO, *Mathematical and Numerical Models for Focal Cerebral Ischemia and Electrocardiology*, PhD thesis, Politecnico di Milano, 2009.
- [22] A. J. PULLAN, L. K. CHENG, M. L. BUIST, AND M. L. B. ANDREW J. PULLAN, LEO K. CHENG, *Mathematically Modelling the Electrical Activity of the Heart*, World Scientific, Singapore, 2005.
- [23] Z. QU AND A. GARFINKEL, *An advanced algorithm for solving partial differential equation in cardiac conduction*, *IEEE Trans. Biomed. Eng.*, 46 (1999), pp. 1166–1168.
- [24] A. QUARTERONI, R. SACCO, AND F. SALERI, *Numerical Mathematics*, Springer, New York, 2000.
- [25] S. RUSH AND H. LARSEN, *A practical algorithm for solving dynamic membrane equations*, *IEEE Trans. Biomed. Eng.*, (1978), pp. 389–392.
- [26] J. SUNDNES, G. T. LINES, AND A. TVEITO, *An operator splitting method for solving the bidomain equations coupled to a volume conductor model for the torso*, *Math. Biosci.*, 194 (2005), pp. 233–248.
- [27] M. VENERONI, *Reaction-diffusion systems for the microscopic cellular model of the cardiac electric field*, *Math. Methods Appl. Sci.*, 29 (2006), pp. 1631–1661.
- [28] ———, *Reaction-diffusion systems for the macroscopic bidomain model of the cardiac electric field*, *Nonlinear Anal. Real World Appl.*, 10 (2009), pp. 849–868.
- [29] H. YU, *A local space-time adaptive scheme in solving two-dimensional parabolic problems based on domain decomposition methods*, *SIAM J. Sci. Comput.*, 23 (2001), pp. 304–322.